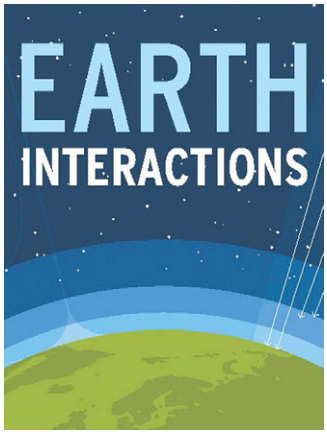

Copyright © 2015, Paper 19-004; 46089 words, 1 Figures, 0 Animations, 12 Tables.
http://EarthInteractions.org

The Hydrometeorology of the Kariba Catchment Area Based on the Probability Distributions

S. Muchuru*

Department of Geography, Geoinformatics and Meteorology, University of Pretoria, Pretoria, South Africa

C. M. Botai

South African Weather Service, Pretoria, South Africa

J. O. Botai and A. M. Adeola

Department of Geography, Geoinformatics and Meteorology, University of Pretoria, Pretoria, South Africa

Received 24 February 2014; accepted 12 November 2014

ABSTRACT: In this paper, monthly, maximum seasonal, and maximum annual hydrometeorological (i.e., evaporation, lake water levels, and rainfall) data series from the Kariba catchment area of the Zambezi River basin, Zimbabwe, have been analyzed in order to determine appropriate probability distribution models of the underlying climatology from which the data were

* Corresponding author address: S. Muchuru, Department of Geography, Geoinformatics and Meteorology, University of Pretoria, Private Bag X20 Hatfield, Pretoria 0028, South Africa.

E-mail address: shephido@yahoo.com; shephido@yahoo.com; christina.botai@weathersa.co.za; joel.botai@up.ac.za; amadeola@yahoo.com

DOI: 10.1175/EI-D-14-0019.1

Unauthenticated | Downloaded 08/05/21 09:27 PM UTC

generated. In total, 16 probability distributions were considered and the Kolmogorov–Sminorv (KS), Anderson–Darling (AD), and chi-square (χ^2) goodness-of-fit (GoF) tests were used to evaluate the best-fit probability distribution model for each hydrometeorological data series. A ranking metric that uses the test statistic from the three GoF tests was formulated and used to select the most appropriate probability distribution model capable of reproducing the statistics of the hydrometeorological data series. Results showed that, for each hydrometeorological data series, the best-fit probability distribution models were different for the different time scales, corroborating those reported in the literature. The evaporation data series was best fit by the Pearson system, the Lake Kariba water levels series was best fit by the Weibull family of probability distributions, and the rainfall series was best fit by the Weibull and the generalized Pareto probability distributions. This contribution has potential applications in such areas as simulation of precipitation concentration and distribution and water resources management, particularly in the Kariba catchment area and the larger Zambezi River basin, which is characterized by (i) nonuniform distribution of a network of hydrometeorological stations, (ii) significant data gaps in the existing observations, and (iii) apparent inherent impacts caused by climatic extreme events and their corresponding variability.

KEYWORDS: Africa; Hydrologic models; Climate variability

1. Introduction

Management of scarce water resources is one of the current and perhaps future critical issues facing African countries. This problem is exacerbated by the unequal geographical distribution of natural resources; accessibility; and unsustainable water usage, which characterizes water supplies from rivers, streams, ocean, lakes, and rainfall. The African continent exhibits some of the driest deserts, largest tropical rain forests and highest equatorial mountains in the world. However, most of the key natural resources are unevenly distributed, including water resources. Climate change has the potential to impose pressure on water availability and accessibility. Climatic warming observed over the past decades is consistently associated with changes in numerous components of the hydrological systems. Such components include changing precipitation patterns, intensity and extremes, widespread melting of snow and ice, increasing atmospheric water vapor, increasing evaporation, and changes in soil moisture and surface runoff. Changes in any of these hydroclimatic variables may alter regional hydrological cycle and systems and subsequently impact the quantity and quality of regional water resources as well as the spatial distribution of water on land.

According to Huang et al. (2013), precipitation is one of the most important climate elements directly affecting the availability of water resources. For example, in northwest China, the impact of climate change on water resources [in the Tarim River basin (TRB)] was reported in Xu et al. (2004). The authors found that precipitation and the streamflow from the headwater of the Tarim River exhibited a 5% level of significant increase. In addition, the authors reported a decreasing trend in the streamflow of the mainstream of the river. In similar studies, Xu et al. (2006) reported that an increasing trend in precipitation was the main reason for the increase of runoff in the headwater catchment of the TRB during the last several decades. Furthermore, Xu et al. (2010) used a Mann–Kendall test to detect the

Unauthenticated | Downloaded 08/05/21 09:27 PM UTC

Table 1. Characteristics of the study variables.

Parameter	Actual time scales	Transformed time scale	Period of series
Rainfall	Monthly	Monthly	1962–2011
		Seasonal maxima	
		Annual maxima	
Lake water level	Daily	Monthly	1960–2007
		Seasonal maxima	
		Annual maxima	
Evaporation	Monthly	Monthly	1962–2011
		Seasonal maxima	
		Annual maxima	

trends of major hydroclimatic variables in the TRB for the period of 1960–2007 and found that both mean annual air temperature and precipitation experienced an increasing trend for the TRB for the past five decades. The authors further concluded that the impact of precipitation on runoff generation was greater than that of air temperature, while the impact of precipitation on actual evaporation amount is less important than that of air temperature. By using correlation and spectral analysis, Jöhnk et al. (2004) detected long-term variability in the time series of lake levels and precipitation derived from two catchments in India. Studies reported in, for example, Chen et al. (2007), Zhao et al. (2010), Kamruzzaman et al. (2013), and Fathian et al. (2015) all demonstrate the effect of changes in climatic variables to hydrology of lake basins.

Various regions of the African continent have suffered from climate (e.g., rainfall) variability on time scales of decades and centuries. Semiarid regions of the Northern Hemisphere exhibit interannual rainfall fluctuations, indicative of a land–atmosphere feedback mechanism (Nicholson 2000). Southern Africa experiences dry or wet periods of varying lengths ranging from days to decades. Rainfall in most of the countries of southern Africa shows a high degree of interannual and intra-annual variability. Such fluctuations, which are also associated with floods and droughts, often raise concern to many climate researchers. As a result, several studies of rainfall variations have focused on spatial and temporal aspects of these variations at different time scales. In southern Africa, most of precipitation occurs during the period November–April with highest peaks during the period December–March (Mulenga 1998); hence, most of the studies have used monthly or seasonal data to investigate interannual variability of precipitation (see, e.g., Tyson 1984, 1986; Matarira and Jury 1992; Levy 1993; and references therein).

Extreme climatic conditions and high interannual or seasonal variability of climatic parameters could adversely affect water resources and agricultural production (Li et al. 2006). The pattern and amount of rainfall are considered the key factors that affect water resources as well as agricultural productivity. Hydrometeorological data (e.g., long-term records of rainfall, evaporation, and lake levels; see Table 1) often provide information about rainfall patterns and its variability (Lazaro et al. 2001). Rainfall patterns are often inferred from computation of probability distribution functions, with a normal distribution function being the most commonly used in rainfall analysis. Despite the wide applicability of the normal distributions there have been other instances though limited when observed distributions from rainfall data analysis were found to be neither normal nor

Unauthenticated | Downloaded 08/05/21 09:27 PM UTC

symmetrical. For example, Jackson (1977) reported that annual rainfall distributions are markedly skewed in semiarid areas, hence contradicting the assumption of normal frequency distribution in such areas.

Rainfall extremes are often described by use of generalized extreme value (GEV) fitted to a block of maxima or blocks of time windows like an annual maxima time series. A number of research studies related to rainfall extremes involving the GEV distribution have been reported in the literature. For example, using GEV distribution, Mannshardt-Shamseldin et al. (2010) developed a family of regression relationships between rain gauge and gridded precipitation data and found that the return values computed from the rain gauge data are typically higher than those computed from gridded precipitation data. Based on the results, the authors concluded that from climate extreme models it is possible to project future changes in precipitation extremes at the point-location level. Wang and Zhang (2008) estimated GEV parameters using extreme daily precipitation data from 1949 to 1999 over North America and found that large-scale circulation exerts a strong influence mostly on location parameters with little values. In a case study at Debre Markos in the northwestern highlands of Ethiopia, Shang et al. (2011) used the GEV modeling to assess the trends on the daily precipitation time series data. In this study, the authors found no evidence to support long-term increasing trend in extreme precipitation at the study location; hence, the null hypothesis that there is no increasing trend in extreme precipitation at that location was accepted.

Generally, the African continent is projected to become warm during this century with the anticipated warmth being larger than the global and annual-mean warming throughout the continent and in all seasons, with drier subtropical regions warming more than the moister tropics. Annual rainfall is anticipated to decrease in much of Mediterranean Africa and the northern Sahara, with the possibility of a decrease in rainfall increase as the Mediterranean coast is approached. In southern Africa, rainfall is projected to decrease in much of the winter rainfall region and on western margins. There is also a high possibility of an increase in annual-mean rainfall in East Africa. Despite these projections, studies focusing on statistical characterization of weather and climate events such as rainfall, precipitation, evaporation, and lake levels particularly in southern Africa are very limited. Extremes of weather and climate events can have devastating effects on human society and the environment. Proper assessment and understanding of past changes in the characteristics of such events is crucial for accurate planning of infrastructure and prevention measures. In addition, since lake levels respond to rainfall as well as to human interference and consumption, it is essential to understand the link between the lakes and their respective catchments. In particular, the Kariba catchment area is a significant hydrometeorological region encompassing Zimbabwe and Zambia (see Figure 1) because it influences agricultural and livestock production systems of the area as well as the general livelihoods of the populace. Furthermore, the Kariba Dam is a major source of hydroelectricity. Just like the other parts of southern Africa, the Kariba catchment area is projected to be highly susceptible to climate change and variability. To further understand the extent of climate change and variability and assess the vulnerability and adaptive capacity of livelihoods in the Kariba catchment area, long-term hydrometeorological observations are a must. The Kariba catchment area has a highly sparse network of hydrometeorological stations with intermittent observations. One way to

Unauthenticated | Downloaded 08/05/21 09:27 PM UTC

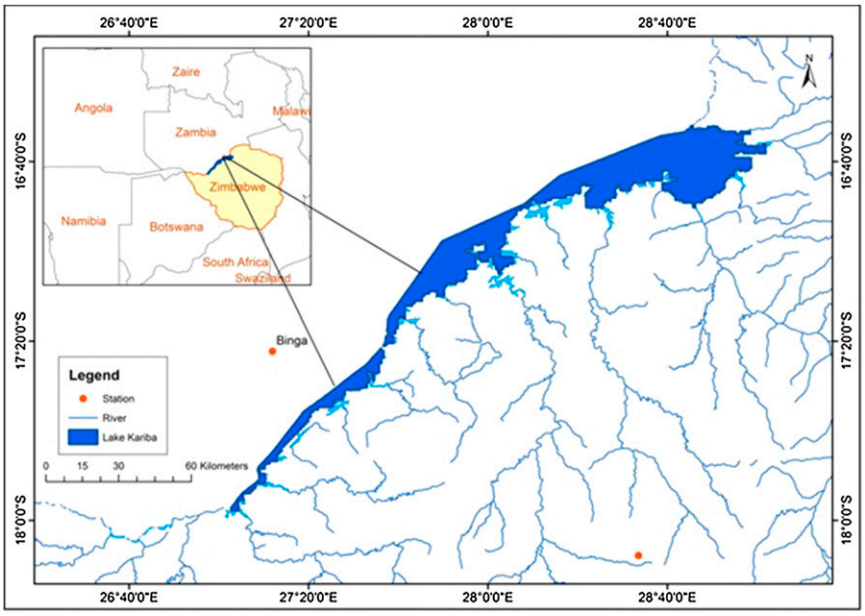

Figure 1. Location of the Lake Kariba River basin.

circumvent the problem of inadequate data span and gaps is to use precipitation generators (see, e.g., Li et al. 2011). One of the principles underpinning precipitation generation is that precipitation amounts often follow certain probability distribution (Li et al. 2013). Therefore, assessing the nature of probability distribution model capable of reproducing statistical moments of hydrometeorological observations could contribute toward long-term series of precipitation generation, which is an important parameter in hydrological modeling, climate change, and variability. The objective is to study climatic characteristics on hydrometeorological data across Lake Kariba by use of a suitable probability distribution function. In sections 2 and 3, the study area and meteorological data used in this study are described, respectively. Section 4 presents the methodology considered in the present study while results and discussion are elucidated in section 5. Section 6 presents the conclusions of the study.

2. Study area

Lake Kariba is located approximately 365 km northwest of Harare in Zimbabwe. Its surface area stretches from the confluence of the Deka and Zambezi Rivers in the southwest, 277 km long and 40 km at its widest point (see Figure 1). The lake has a catchment area of 663 848 km^2 (18°04′S, 26°42′E) to the Kariba Gorge (16°31′S, 28°45′E) in the northeast and extends over parts of Angola, Zambia, Namibia, Botswana, and Zimbabwe. The lake is bordered by Zambia in the north and Zimbabwe in the south and has generally a southwest–northeast orientation. It forms part of the Zambezi basin, which has a vast catchment of 1 193 500 km^2 and includes the states of Mozambique and Malawi. Lake Kariba regulates runoff from

Unauthenticated | Downloaded 08/05/21 09:27 PM UTC

an upstream catchment area of 687 535 km^2, which is about 50% of the total Zambezi catchment area. The climate of Kariba is typically tropical and semiarid, with four distinct seasons in the Gwembe valley, where the lake is located. These seasons are described as rainy (November–February), postrainy (March–May), dry and cool winter (June–July), and dry and hot (August–October). Air temperatures are consistently high with a mean annual temperature ranging from 24.4° to 24.7°C. Maximum monthly air temperatures occur during the dry and hot season, averaging 30.70°C, with those during the cold winter season averaging 21.71°C. Average annual rainfall for the Lake Kariba catchment is about 1000 mm, producing a mean annual discharge of 37 249 Mm^3 (an average flow rate of 1181 m^3 s^{-1}). The El Niño–Southern Oscillation and the intertropical convergence zone (ITCZ) are the major factors that influence the unimodal rainfall in the Zambezi basin, which occurs from November to March/April in response to the movements of the ITCZ.

3. Catchment data

Observed monthly, seasonal, and annual time series of precipitation, lake water levels and evaporation, were used to estimate monotonic trends of these variables. The variables were obtained from various sources, including the Zimbabwe Meteorological Services (ZMS) and Zambezi River Authority (ZRA). Monthly observations of the selected variables with continuous data series from 1962 to 2011 were selected in this study. The period of study on lake water level time series was limited to 1960–2007, since level data after 2007 have not been released by related water authorities. In this paper, extreme hydrometeorological data series were considered. First, the annual maximum precipitation, lake levels, and evaporation were derived from the monthly data series during 1960–2010. Second, the seasonal maximum precipitation, lake levels, and evaporation were derived from the November, December, January, February, and March data subset. Deriving seasonal maximum values from a 5-month dataset was motivated by presence of an intra-annual pattern of precipitation characteristic of the study area.

4. Method of data analysis

The probability distributions, given in Table 2, were evaluated for the best-fit probability distribution model suitable for hydrometeorology datasets $\{Y\}_{i=1,2,3,\ldots,N}$ for the Kariba catchment area. In the research work reported in this contribution, the parameters of the different distributions have been estimated by use of the maximum-likelihood estimators (MLEs). For detailed discussion of MLEs, see Hosking et al. (1985). Overall, the probability distribution model that best fits the hydrometeorological data was accomplished based on the following:

1) For each hydrometeorological series, different probability distributions were fitted and the MLE was used to estimate the corresponding parameters.
2) A goodness-of-fit (GoF) test (i.e., measure the compatibility of each hydrometeorological data series with the theoretical probability distribution) was performed using the Kolmogorov–Sminorv (KS), Anderson–Darling (AD), and chi-square (CS) GoF tests at α level of significance [see, e.g., Ricci (2005) for details on the KS, AD, and CS]. In all the tests, the

Unauthenticated | Downloaded 08/05/21 09:27 PM UTC

null hypothesis used was H_0 when the hydrometeorological dataset follows a specified distribution and H_1 when the hydrometeorological dataset does not follow a specified distribution. For each hydrometeorological data series, the best-fit probability distribution model was identified based on the following algorithm:

(i) The different GoF test statistic was used to rank the probability distributions considered. Here, the sum of the test statistic from the three GoFs was computed for each probability distribution model. The resulting sums of GoFs for each probability distribution model were then sorted in ascending order. The highest ranked distribution considered was one with the minimum sum of the test statistic. The first three ranked probability distribution models were selected.

(ii) To obtain a suitable probability distribution model for a particular hydrometeorology dataset from the triad (the three best ranked probability distribution models), the corresponding probability distribution model parameters are used to generate surrogate data series $\{G\}_{i=1,2,3,\ldots,N}$. The residuals $\{R\}_{j=1,2,3}$ computed from

$$R_j = \left| \sum_{i=1}^{n} (Y_i - G_i) \right| \tag{1}$$

are assessed. A distribution with $\min\{R\}$ is considered to be the best-fit probability distribution model for the hydrometeorology series.

5. Results and discussion

5.1. Temporal variability of Kariba catchment hydrometeorological data

The hydrometeorological maxima datasets (i.e., rainfall, evaporation, and Lake Kariba water levels) used in this study were classified into (i) annual, (ii) seasonal, and (iii) monthly data series. Statistical moments characterizing each of the datasets are presented in Table 3. Monthly rainfall time series has the highest variation (i.e., largest standard deviation) with the lowest mean value and highest positive skewness demonstrating that the monthly time series is substantially asymmetrical with a long tail to the right. The skewness of the rainfall time series decreases from fine temporal scales to coarse temporal scales. Therefore, the inherent asymmetry of the rainfall distribution in the Kariba catchment is dependent on the observational time scales. The largest kurtosis value in monthly rainfall time series is an indicative of high probability of extreme rainfall values in the monthly datasets. The observed kurtosis in the rainfall series decreases with decreasing temporal resolution. At all time scales, the Kariba catchment rainfall series exhibit nonsignificant negative trend. Further, the annual precipitation concentration index (PCI) described in, for example, De Luis et al. (2011) and Valli et al. (2013) is also used to characterize the heterogeneity in monthly rainfall over the Kariba catchment area. From our analysis, 22% of the monthly rainfall series had irregular

Unauthenticated | Downloaded 08/05/21 09:27 PM UTC

Table 2. Probability distribution functions.

Name of the distribution	Probability density function	Parameter
Chi squared	$f(x) = \dfrac{x^{(\upsilon/2)-1}}{\Gamma\left(\dfrac{\upsilon}{2}\right)2^{(\upsilon/2)}} e^{(-x)/2}$	$\upsilon(x > 0)$: degrees of freedom; γ: noncentering parameter
Chi squared (2P)	$f(x) = \dfrac{(x-\gamma)^{(\upsilon/2)-1}}{\Gamma\left(\dfrac{\upsilon}{2}\right)2^{\upsilon/2}} e^{[-(x-\gamma)]/2}$	
Gamma (2P)	$f(x) = \dfrac{\beta^{-\xi}x^{\xi-1}}{\Gamma(\xi)} e^{(-x)/\beta}$	ξ (>0): shape parameter; β (>0): scale parameter; γ: location parameter [≡0; ≥2P gamma (Γ) distribution]
Gamma (3P)	$f(x) = \dfrac{\beta^{-\xi}(x-\gamma)^{\xi-1}}{\Gamma(\xi)} e^{(-x+\gamma)/\beta},\ \gamma \le x < +\infty$	
Log gamma	$f(x) = \dfrac{x^{-1}\beta^{-\xi}[\ln(x)]^{\xi-1}}{\Gamma(\xi)} e^{\{-[\ln(x)]\}/\beta},\ 0 \le x < +\infty$	ξ (>0): shape parameter; β (>0): scale parameter
Generalized extreme value	$f(x) = \dfrac{1}{\beta}[1+\xi\kappa]^{-[(\xi+1)/\xi]} e^{-[1+\xi\kappa]^{-(1/\xi)}};\ (1+\xi\kappa) > 0;\ \kappa = \dfrac{x-\gamma}{\beta}$	ξ: shape parameter; β (>0): scale parameter; γ: location parameter
Generalized Pareto (3P)	$f(x) = \dfrac{1}{\beta}[1+\xi\kappa]^{-[(\xi+1)/\xi]};\ \mu \le x;\ x \le \mu - \dfrac{\beta}{\xi}$	ξ (>0): shape parameter; β (>0): scale parameter; μ: threshold
Lognormal (2P)	$f(x) = \dfrac{e^{-\{[\ln(x)-\xi]/4\beta\}^2}}{x\beta\sqrt{2\pi}}$	ξ (>0): shape parameter; β (>0): scale parameter; γ: location parameter (≡0; ≥2P lognormal distribution)
Lognormal (3P)	$f(x) = \dfrac{e^{-\{[\ln(x-\gamma)-\xi]/4\beta\}^2}}{(x-\gamma)\beta\sqrt{2\pi}},\ \gamma < x < +\infty$	

Unauthenticated | Downloaded 08/05/21 09:27 PM UTC

Table 2. (*Continued*)

Name of the distribution	Probability density function	Parameter
Pearson 5 (2P)	$f(x) = \dfrac{e^{-(\beta/x)}}{\beta\Gamma(\xi)\left(\dfrac{x}{\beta}\right)^{\xi+1}}$	ξ (>0): shape parameter; β (>0): scale parameter; γ: location parameter (≡0, ≥2P Pearson 5 distribution)
Pearson 5 (3P)	$f(x) = \dfrac{e^{-[\beta/(x-\gamma)]}}{\beta\Gamma(\xi)\left(\dfrac{(x-\gamma)}{\beta}\right)^{\xi+1}}$, $\gamma < x < +\infty$	
Pearson 6 (3p)	$f(x) = \dfrac{\beta^{\xi_1-1}x^{\xi_1-1}}{\beta\mathrm{B}(\xi_1, \xi_2)\left(1+\dfrac{x}{\beta}\right)^{\xi_1+\xi_2}}$	ξ_1 (>0), ξ_2 (>0): shape parameters; β (>0): scale parameter; γ: location parameter (≡0; ≥3P Pearson 6 distribution)
Pearson 6 (4P)	$f(x) = \dfrac{\beta^{\xi_1-1}(x-\gamma)^{\xi_1-1}}{\beta\mathrm{B}(\xi_1, \xi_2)\left(1+\dfrac{x-\gamma}{\beta}\right)^{\xi_1+\xi_2}}$, $\gamma \le x < +\infty$	
Weibull (2P) Weibull (3)	$f(x) = \beta^{-1}\xi(\beta^{-1}x)^{\xi-1}e^{-(\beta^{-1}x)^{\xi}}$ $f(x) = \beta^{-1}\xi[\beta^{-1}(x-\gamma)]^{\xi-1}e^{-[\beta^{-1}(x-\gamma)]^{\xi}}$, $\gamma \le x < +\infty$	α (>0): shape parameter; β (>0): scale parameter; γ: location parameter (≡0; ≥2P Weibull distribution)

Unauthenticated | Downloaded 08/05/21 09:27 PM UTC

Table 3. Summary of the statistics of Kariba catchment hydrometeorological data: *N*(0) is insignificant negative trend; N(1) is significant negative trend; P(0) is insignificant positive trend; and P(1) is significant positive trend.

Dataset		Statistical parameters					
		Min/max	Mean	Std dev	Skewness	Kurtosis	Trend (significance test)
Rainfall (mm)	Annual	84/451	243.93	76.09	0.17	0.06	N(0)
	Seasonal	71/451	242.62	71.73	0.24	0.60	N(0)
	Monthly	0/451	61.11	86.12	1.52	1.62	N(0)
Evaporation (mm)	Annual	171/254	205.35	17.12	0.44	1.04	P(0)
	Seasonal	139/254	191.30	24.11	0.08	0.91	P(1)
	Monthly	84/264	142.92	33.79	0.57	−0.23	P(0)
Lake levels (m)	Annual	472.07/487.84	483.63	3.35	−0.94	1.39	N(0)
	Seasonal	463.58/487.42	482.23	4.19	−2.04	7.38	N(0)
	Monthly	460.85/487.84	482.19	3.98	−1.85	6.68	N(1)

distribution (i.e., the PCI values range was 10–15) while 78% of the monthly rainfall series exhibited strong irregularity (i.e., $16 \leq \text{PCI} \leq 20$). Overall, monthly rainfall series in the Kariba catchment area is highly varied.

The statistical moments in evaporation time series demonstrate a dependence of the temporal resolution. Monthly/annual maxima evaporation time series exhibit the highest/lowest standard deviation. Furthermore, the high positive skewness in the observed monthly/annual maxima evaporation time series demonstrates a significant asymmetry with a long tail to the right. The asymmetry in the maximum seasonal evaporation is not substantial. In general, based on the evaporation time series considered in this study, it is unclear whether the asymmetry is time scale dependent. For kurtosis, annual maximum and seasonal maximum evaporation time series exhibit high positive values, suggesting that the evaporation time series exhibit leptokurtic properties at these time scales. As a result, the presence of extreme values in annual and seasonal maximum evaporation time series is highly probable. On the other hand, monthly evaporation time series exhibit negative kurtosis, signifying that the evaporation time series is relatively flat compared to a normal distribution. In addition, the evaporation time series exhibits positive trends that were insignificant except for the seasonal maximum evaporation time series.

The temporal variability of lake water level time series in the Kariba catchment is not highly pronounced based on the first and second moments given in Table 3. The lake water level time series exhibit negative skewness at all the time scales of the series considered in the present analysis. The negative skewness in lake water levels imply a substantial asymmetry with a long tail to the left (or the mean and median are less than the mode), indicating that extreme values lie toward the negative end of the distribution (small lake water levels records). The monthly lake water levels exhibit high positive kurtosis suggesting that the series is leptokurtic. Overall, the fourth statistical moment of lake water level time series is dependent on the time scale of observation with the probability of extreme values being present decreasing with a decrease in the time scales. The lake water levels have inherent nonsignificant negative trends at annual and seasonal time scales with a negative significant trend in the monthly series.

Unauthenticated | Downloaded 08/05/21 09:27 PM UTC

Table 4. Goodness-of-fit results for the annual maximum evaporation data. The top reranked distributions are in bold.

No.	Distribution	Kolmogorov–Smirnov		Anderson–Darling		Chi squared		Sum of the 3 ranks	Weighted sum	Reranked
		Statistic	Rank	Statistic	Rank	Statistic	Rank			
1	Chi squared	0.11	13	0.87	12	3.14	13	38	84.44	13
2	Chi squared (2P)	0.08	9	0.38	9	2.45	12	30	66.67	11
3	Gamma	0.08	10	0.38	8	0.67	1	19	42.22	7
4	Gamma (3P)	0.07	6	0.38	6	2.20	4	16	35.56	5
5	GEV	0.08	8	0.43	10	2.17	3	21	46.67	8
6	Generalized Pareto	0.11	14	12.18	15	N/A	N/A	29	96.67	15
7	Log gamma	0.08	7	0.37	5	2.22	11	23	51.11	9
8	**Lognormal**	**0.07**	**3**	**0.36**	**1**	**2.21**	**9**	**13**	**28.89**	**3**
9	Lognormal (3P)	0.07	4	0.37	4	2.20	6	14	31.11	4
10	**Pearson 5**	**0.07**	**1**	**0.37**	**2**	**2.20**	**8**	**11**	**24.44**	**1**
11	Pearson 5 (3P)	0.07	5	0.38	7	2.20	5	17	37.78	6
12	Pearson 6	0.18	15	2.20	14	12.59	14	43	95.56	14
13	**Pearson 6 (4P)**	**0.07**	**2**	**0.37**	**3**	**2.20**	**7**	**12**	**26.67**	**2**
14	Weibull	0.10	12	1.00	13	1.63	2	27	60.00	10
15	Weibull (3)	0.08	11	0.50	11	2.21	10	32	71.11	12

5.2. Assessment of the probability distribution and goodness of fit

5.2.1. Probability distribution and goodness-of-fit models for annual maxima hydrometeorological data

In this study, 16 probability distribution functions were fitted to annual maximum evaporation, lake water levels and rainfall time series over the Kariba catchment. Tables 4–6 list the summary of the distribution parameters, the statistic for the GoF tests [based on the Kolmogorov–Sminorv, Anderson–Darling, and chi-square (χ^2) tests], the ranking of the distribution based on individual GoF tests, and

Table 5. Goodness-of-fit results for the annual maximum lake levels data, where the top reranked distributions are in bold. (NaN: not a number.)

No.	Distribution	Kolmogorov–Smirnov		Anderson–Darling		Chi squared		Sum of the 3 ranks	Weighted sum	Reranked
		Statistic	Rank	Statistic	Rank	Statistic	Rank			
1	Chi squared	0.43	11	13.85	11	143.29	10	32.00	71.11	12
2	Chi squared (2P)	0.19	10	3.09	9	8.16	9	28.00	62.22	11
3	**Gamma**	**0.12**	**4**	**0.92**	**3**	**3.91**	**4**	11.00	24.44	**3**
4	Gamma (3P)	0.12	7	0.96	6.00	4.52	6.00	19.00	42.22	6
5	**GEV**	**0.08**	**1**	**0.58**	**1**	**0.89**	**1**	3.00	6.67	**1**
6	Generalized Pareto	0.09	3.00	4.30	10.00	NaN	NaN	13.00	43.33	7
7	Log gamma	**0.12**	**5**	**0.92**	**4**	**3.90**	**3**	12.00	26.67	**4**
8	**Lognormal**	**0.12**	**6**	**0.93**	**5**	**3.94**	**5**	16.00	35.56	**5**
9	**Lognormal (3P)**	0.12	8	0.97	7	5.46	8	23.00	51.11	8
10	**Pearson 5**	1.00	14	NaN	NaN	NaN	NaN	NaN	NaN	NaN
11	Pearson 5 (3P)	0.12	9	1.01	8	5.45	7	24.00	53.33	9
12	Pearson 6	0.48	12	15.63	12	299.96	11	35.00	77.78	13
13	**Pearson 6 (4P)**	0.50	13	18.35	13	N/A	N/A	26.00	57.78	10
14	**Weibull**	**0.09**	**2**	**0.66**	**2**	**1.66**	**2**	6.00	13.33	**2**
15	Weibull (3)	NaN	NaN	NaN		NaN	NaN	NaN	NaN	NaN

Unauthenticated | Downloaded 08/05/21 09:27 PM UTC

Table 6. Goodness-of-fit results for annual maximum rainfall data. The top reranked distributions are in bold.

No.	Distribution	Kolmogorov–Smirnov		Anderson–Darling		Chi squared		Sum of the 3 ranks	Weighted sum	Reranked
		Statistic	Rank	Statistic	Rank	Statistic	Rank			
1	Chi squared	0.300	15	50.513	15	38.457	14	44	97.78	15
2	**Chi squared (2P)**	**0.067**	**2**	**0.184**	**1**	**1.329**	**8**	11	24.44	**3**
3	Gamma	0.099	9	0.440	9	1.206	7	25	55.56	9
4	Gamma (3P)	0.076	5	0.226	6	1.435	10	21	46.67	8
5	**GEV**	**0.065**	**1**	**0.206**	**3**	**0.773**	**4**	8	17.78	**2**
6	Generalized Pareto	0.102	10	7.948	14	N/A	N/A	24	80.00	12
7	Log gamma	0.134	13	0.799	12	2.071	12	37	82.22	13
8	Lognormal	0.125	12	0.673	11	2.032	11	34	75.56	11
9	Lognormal (3P)	0.071	3	0.207	4	1.401	9	16	35.56	5
10	Pearson 5	0.150	14	1.050	13	7.726	13	40	88.89	14
11	Pearson 5 (3P)	0.082	6	0.254	7	0.803	5	18	40.00	6
12	Pearson 6	0.103	11	0.452	10	1.205	6	27	60.00	10
13	Pearson 6 (4P)	0.089	8	0.304	8	0.500	3	19	42.22	7
14	**Weibull**	**0.082**	**7**	**0.222**	**5**	**0.361**	**2**	14	31.11	**4**
15	**Weibull (3)**	**0.075**	**4**	**0.201**	**2**	**0.220**	**1**	7	15.56	**1**

the reranking based on the minimum deviation between the actual and randomly generated series of each of the three probability distributions for each hydrometeorology data.

For annual maximum evaporation time series, the probability distributions that had a better capability to reproduce the empirical cumulative distribution (i.e., those ranked first by individual GoF tests) were gamma using χ^2, lognormal using AD, and Pearson 5 using the KS GoF tests. On the other hand, the GEV was ranked first by all the three GoF tests on the annual maximum lake water level time series. For annual rainfall maximum time series, the two-parameter χ^2 (using AD test) distribution, the GEV (using the KS test), and the three-parameter Weibull distribution (using the χ^2 test) were the most probable distributions functions that could reproduce the annual rainfall empirical cumulative distribution.

5.2.2. Probability distribution and goodness-of-fit seasonal hydrometeorological data

The seasonal maxima evaporation, lake water level, and rainfall time series were fitted with 16 probability distributions functions, ranked individually across the KS, AD, and χ^2 GoF tests as well as by use of the minimum deviation between the actual observations and the proxy series generated from the selected distribution parameters. Tables 7–9 provide a summary of the test statistic, the rank, and reranking results. Table 7 illustrates that the seasonal time series of evaporation is best fit by the χ^2 and the four-parameter Pearson 6 distribution based on the KS and AD GoF tests. As depicted in Table 8, the GEV distribution is considered to be a best-fit model to the seasonal maximum lake water level series based on the KS and AD GoF tests while the Weibull distribution could produce a better empirical cumulative distribution according to the χ^2 GoF test. The GoF tests depicted in Table 9 demonstrate that the seasonal maximum rainfall time series could be better fit by the two-parameter χ^2 distribution according to KS and AD GoF tests.

Unauthenticated | Downloaded 08/05/21 09:27 PM UTC

Table 7. Goodness-of-fit results for seasonal evaporation data. The top reranked distributions are in bold.

No.	Distribution	Kolmogorov–Smirnov Statistic	Kolmogorov–Smirnov Rank	Anderson–Darling Statistic	Anderson–Darling Rank	Chi squared Statistic	Chi squared Rank	Sum of the 3 ranks	Weighted sum	Reranked
1	**Chi squared**	**0.08**	**1**	**1.09**	**12**	**1.67**	**1**	14	31.11	**2**
2	Chi squared (2P)	0.12	10	0.84	4	5.16	6	20	44.44	11
3	Gamma	0.12	7	0.86	6	5.16	5	18	40.00	6
4	Gamma (3P)	0.12	8	0.84	3	5.18	8	19	42.22	8
5	**GEV**	**0.11**	**4**	**0.90**	**7**	**3.03**	**3**	14	31.11	**2**
6	Generalized Pareto	0.16	14	16.23	15			29	96.67	15
7	Log gamma	0.13	12	1.02	11	6.72	12	35	77.78	12
8	Lognormal	0.13	11	0.96	9	6.67	11	31	68.89	10
9	**Lognormal (3P)**	**0.11**	**5**	**0.78**	**2**	**5.88**	**9**	16	35.56	**5**
10	Pearson 5	0.13	13	1.10	13	6.76	13	39	86.67	13
11	Pearson 5 (3P)	0.12	6	0.84	5	5.17	7	18	40.00	6
12	Pearson 6	0.22	15	3.79	14	16.32	14	43	95.56	14
13	**Pearson 6 (4P)**	**0.11**	**3**	**0.76**	**1**	**3.18**	**4**	8	17.78	**1**
14	**Weibull**	**0.11**	**2**	**0.98**	**10**	**2.32**	**2**	14	31.11	**2**
15	Weibull (3)	0.12	9	0.91	8	6.06	10	27	60.00	10

Overall, using the reranking procedure described in section 4, the distribution pattern of the maximum seasonal evaporation, lake water levels, and rainfall time series over the Kariba catchment area can be characterized by four-parameter Pearson 6, the GEV, and the two-parameter χ^2 distribution, respectively.

5.2.3. Probability distribution and goodness-of-fit extreme monthly hydrometeorological data

Tables 10–12 have a summary of the fitted probability distribution statistic and the ranking based on the KS, AD, and χ^2 GoF tests. In particular, given in Table 10

Table 8. Goodness-of-fit results for seasonal lake levels data, where the top reranked distributions are in bold. (NaN: not a number.)

No.	Distribution	Kolmogorov–Smirnov Statistic	Kolmogorov–Smirnov Rank	Anderson–Darling Statistic	Anderson–Darling Rank	Chi squared Statistic	Chi squared Rank	Sum of the 3 ranks	Weighted sum	Reranked
1	Chi squared	0.42	11.00	13.64	10.00	44.37	10.00	31	68.89	13
2	Chi squared (2P)	0.23	10.00	4.43	9.00	15.49	9.00	28	62.22	12
3	**Gamma**	**0.15**	**5.00**	**1.36**	**4.00**	**3.58**	**7.00**	16	35.56	**4**
4	Gamma (3P)	0.15	8.00	1.52	7.00	3.57	5.00	20	44.44	8
5	**GEV**	**0.08**	**1.00**	**0.39**	**1.00**	**3.46**	**2.00**	4	8.89	**1**
6	Generalized Pareto	0.13	3.00	15.16	11.00	NaN	NaN	14	46.67	9
7	Log gamma	0.15	6.00	1.40	6.00	3.57	6.00	18	40.00	5
8	Lognormal	0.15	7.00	1.37	5.00	3.58	8.00	20	44.44	6
9	**Lognormal (3P)**	**0.14**	**4.00**	**1.29**	**3.00**	**3.56**	**4.00**	11	24.44	**3**
10	Pearson 5	1.00	14.00	NaN	NaN	NaN	NaN	14	46.67	9
11	Pearson 5 (3P)	0.16	9.00	1.63	8.00	3.55	3.00	20	44.44	7
12	Pearson 6	0.47	12.00	15.66	12.00	115.33	11.00	35	77.78	14
13	Pearson 6 (4P)	0.57	13.00	18.35	13.00	—	—	26	57.78	11
14	**Weibull**	**0.12**	**2.00**	**1.05**	**2.00**	**3.17**	**1.00**	5	11.11	**2**
15	Weibull (3)	NaN	NaN	NaN	NaN	NaN	NaN	NaN	NaN	15

Unauthenticated | Downloaded 08/05/21 09:27 PM UTC

Table 9. Goodness-of-fit results for seasonal rainfall data. The top reranked distributions are in bold.

No.	Distribution	Kolmogorov–Smirnov		Anderson–Darling		Chi squared		Sum of the 3 ranks	Weighted sum	Reranked
		Statistic	Rank	Statistic	Rank	Statistic	Rank			
1	Chi squared	0.2845	15	42.164	15	49.24	14	44	97.78	15
2	**Chi squared (2P)**	**0.057 17**	**1**	**0.1551**	**1**	**1.264**	**1**	3	6.67	**1**
3	Gamma	0.084 72	9	0.302 19	9	3.9022	9	27	60.00	9
4	**Gamma (3P)**	**0.063 86**	**5**	**0.164 11**	**3**	**1.3348**	**4**	12	26.67	**3**
5	**GEV**	**0.066 88**	**7**	**0.1996**	**6**	**1.285**	**2**	15	33.33	**4**
6	Generatized Pareto	0.109 77	13	8.0943	14	N/A	N/A	27	90.00	14
7	Log gamma	0.105 85	12	0.727 39	12	5.2986	12	36	80.00	12
8	Lognormal	0.099 55	11	0.5995	11	5.1878	11	33	73.33	11
9	**Lognormal (3P)**	**0.0598**	**2**	**0.158 18**	**2**	**1.3244**	**3**	7	15.56	**2**
10	Pearson 5	0.117 02	14	1.0845	13	9.9463	13	40	88.89	13
11	Pearson 5 (3P)	0.065 54	6	0.171 09	4	1.3528	5	15	33.33	4
12	Pearson 6	0.088 34	10	0.328 13	10	3.9275	10	30	66.67	10
13	Pearson 6 (4P)	0.0632	4	0.171 79	5	1.3565	6	15	33.33	4
14	Weibull	0.060 31	3	0.259 13	8	1.5198	8	19	42.22	7
15	Weibull (3)	0.069 34	8	0.215 33	7	1.4076	7	22	48.89	8

are the ranked GoF tests for the monthly evaporation time series. The KS and AD GoF tests rank Weibull as the most suitable distribution capable of reproducing the empirical cumulative distribution intrinsic in the evaporation monthly time series. Along with the overall reranking, the three-parameter gamma distribution is determined as a candidate for best fit to the monthly evaporation time series by using the χ^2 statistic. As for the monthly lake water levels time series, the GEV distribution is reranked first along with the individual KS and AD GoF tests. However, according to the χ^2 GoF test, the Weibull distribution is determined to be a better fit to the monthly the Lake levels series. Based on the KS, AD, and χ^2 GoF tests, the generalized Pareto distribution is determined to be capable to reproduce the

Table 10. Goodness-of-fit results for long-term evaporation data. The top reranked distributions are in bold. (NaN: not a number.)

No.	Distribution	Kolmogorov–Smirnov		Anderson–Darling		Chi squared		Sum of the 3 ranks	Weighted sum	Reranked
		Statistic	Rank	Statistic	Rank	Statistic	Rank			
1	Chi squared	0.22	15.00	147.53	15.00	521.48	14.00	44	97.78	15
2	Chi squared	0.07	13.00	4.42	12.00	25.28	12.00	37	82.22	13
3	Chi squared (2P)	0.06	12.00	2.33	11.00	13.15	2.00	25	55.56	9
4	**Gamma**	**0.05**	**3.00**	**1.15**	**2.00**	**14.87**	**3.00**	8	17.78	**2**
5	**Gamma (3P)**	**0.04**	**2.00**	**1.44**	**3.00**	**10.65**	**1.00**	6	13.33	**1**
6	**GEV**	0.05	6.00	80.98	14.00	NaN	NaN	20	66.67	12
7	Generalized Pareto	0.05	4.00	1.76	8.00	20.25	11.00	23	51.11	8
8	Log gamma	0.05	10.00	1.96	9.00	17.52	9.00	28	62.22	10
9	Lognormal	**0.05**	**7.00**	**1.55**	**4.00**	**16.16**	**5.00**	16	35.56	**4**
10	Lognormal (3P)	0.05	5.00	1.71	7.00	16.58	6.00	18	40.00	5
11	Pearson 5	0.05	8.00	1.70	6.00	16.92	7.00	21	46.67	7
12	Pearson 5 (3P)	0.05	11.00	1.98	10.00	17.40	8.00	29	64.44	11
13	Pearson 6	0.05	9.00	1.65	5.00	15.91	4.00	18	40.00	5
14	Pearson 6 (4P)	0.10	14.00	12.22	13.00	64.31	13.00	40	88.89	14
15	**Weibull**	**0.04**	**1.00**	**0.78**	**1.00**	**20.06**	**10.00**	**12**	**26.67**	**3**

Unauthenticated | Downloaded 08/05/21 09:27 PM UTC

Table 11. Goodness-of-fit results for long-term lake levels data. The top reranked distributions are in bold. (NaN: not a number.)

No.	Distribution	Kolmogorov–Smirnov		Anderson–Darling		Chi squared		Sum of the 3 ranks	Weighted sum	Reranked
		Statistic	Rank	Statistic	Rank	Statistic	Rank			
1	Chi squared	0.42	12.00	164.31	11.00	2518.40	11.00	34	75.56	13
2	Chi squared (2P)	0.21	11.00	55.08	10.00	294.68	10.00	31	68.89	12
3	**Gamma**	**0.09**	**3.00**	**10.17**	**3.00**	**51.80**	**3.00**	9	20.00	**3**
4	Gamma (3P)	0.09	6.00	12.19	7.00	57.30	7.00	20	44.44	8
5	**GEV**	**0.05**	**1.00**	**1.71**	**1.00**	**42.70**	**2.00**	4	8.89	**1**
6	Generalized Pareto	0.10	9.00	216.07	13.00	NaN	NaN	22	48.89	9
7	Log gamma	0.09	5.00	10.50	5.00	54.29	5.00	15	33.33	6
8	**Lognormal**	**0.09**	**4.00**	**10.45**	**4.00**	**52.85**	**4.00**	12	26.67	**4**
9	Lognormal (3P)	0.09	7.00	11.15	6.00	56.45	6.00	19	42.22	7
10	Pearson 5	1.00	14.00	NaN	NaN	NaN	NaN	14	31.11	5
11	Pearson 5 (3P)	0.10	8.00	13.89	9.00	60.75	8.00	25	55.56	10
12	Pearson 6	0.47	13.00	188.42	12.00	5081.70	12.00	37	82.22	14
13	Pearson 6 (4P)	0.10	10.00	12.65	8.00	64.96	9.00	27	60.00	11
14	**Weibull**	**0.06**	**2.00**	**3.56**	**2.00**	**38.71**	**1.00**	5	11.11	**2**
15	Weibull (3)	NaN	NaN	NaN	NaN	NaN	NaN	NaN	NaN	NaN

empirical cumulative distribution inherent in the monthly rainfall totals over the Kariba catchment area.

5.3. Appropriate probability distributions for evaporation, lake levels, and rainfall

Section 5.2 presented a methodology to select a set of probability distributions from a set of 16 probability distributions capable of reproducing key properties of evaporation, Lake Kariba water levels, and a rainfall series in Kariba catchment. In this section, we assess the most appropriate general (family) probability distribution capable of mimicking the statistical moment for each of the data series. The performance of each of the selected family of probability distribution models is assessed through comparison of the regenerated statistical moments derived from the randomly generated empirical data and the actual observations. For an evaporation maxima time series, the Pearson system of probability distributions (e.g., Pearson 5: two, three, and four parameters) is considered to be capable of reproducing the inherent statistics. For rainfall maxima series, the appropriate probability distributions are Weibull family as well as the GEV probability distribution. Additionally, the Weibull family of probability distributions was considered the most appropriate distribution capable of reproducing the statistical moments of the Lake Kariba water levels.

6. Conclusions

One way to understand the fundamental underlying phenomena is to assess it by a probability distribution model, which mimics the statistical moments of the underlying process or phenomena. The practice of fitting probability distribution models to hydrometeorological data has been reported in the literature. In all these

Unauthenticated | Downloaded 08/05/21 09:27 PM UTC

Table 12. Goodness-of-fit results for long-term rainfall data. (NaN: not a number.)

No.	Distribution	Kolmogorov–Smirnov		Anderson–Darling		Chi squared		Sum of the 3 ranks	Weighted sum	Reranked
		Statistic	Rank	Statistic	Rank	Statistic	Rank			
1	Chi squared	0.60	14.00	7620.40	14.00	2269.80	14.00	42	93.33	14
2	Chi squared (2P)	0.56	13.00	4662.00	13.00	2226.90	13.00	39	86.67	13
3	**Gamma**	**0.37**	**3.00**	**93.02**	**3.00**	**567.56**	**3.00**	9	20.00	**3**
4	Gamma (3P)	0.38	6.00	302.82	8.00	885.61	4.00	18	40.00	5
5	**GEV**	**0.23**	**2.00**	**44.67**	**2.00**	**223.30**	**2.00**	6	13.33	**2**
6	**Generalized Pareto**	**0.21**	**1.00**	**35.96**	**1.00**	**152.11**	**1.00**	3	6.67	**1**
7	Log gamma	0.40	9.00	315.90	10.00	993.12	9.00	28	62.22	9
8	Lognormal	0.40	10.00	315.90	11.00	993.13	10.00	31	68.89	12
9	Lognormal (3P)	0.40	11.00	286.96	5.00	1059.30	11.00	27	60.00	8
10	Pearson 5	0.40	12.00	286.96	6.00	1059.30	12.00	30	66.67	11
11	Pearson 5 (3P)	0.38	5.00	302.81	7.00	885.95	6.00	18	40.00	5
12	Pearson 6	0.38	7.00	302.84	9.00	885.74	5.00	21	46.67	7
13	**Pearson 6 (4P)**	**0.37**	**4.00**	**112.70**	**4.00**	**906.87**	**7.00**	15	33.33	**4**
14	Weibull	0.39	8.00	322.91	12.00	913.65	8.00	28	62.22	9
15	Weibull (3)	NaN	NaN	NaN	NaN	NaN	NaN	NaN	NaN	NaN

studies, different probability distributions models were found to be best fit to, for example, rainfall series at specific watershed, catchment, or even point observations (Chapman 1997; Wan et al. 2005; Li et al. 2013). It is therefore apparent that finding a suitable probability distribution model for a hydrometeorological data series is 1) location dependent and 2) highly dependent on temporal scales. In this paper, monthly, maximum seasonal, and annual hydrometeorological (i.e., evaporation, lake water levels, and rainfall) data series from the Kariba catchment area, Zimbabwe, have been analyzed in order to determine appropriate probability distribution models of the underlying climatology from which the data were generated. In particular, 16 probability distributions generally composed of the Weibull family, the Pearson, and the Johnson systems of probability distributions were considered in the analysis. The KS, AD, and χ^2 GoF tests were used to evaluate the best-fit probability distribution model for each hydrometeorological data series. A ranking metric that uses the test statistic from the three GoF tests was formulated and used to select the most appropriate probability distribution model capable of reproducing the statistics of the hydrometeorological data series. The ranking metric considered in the present analysis ensured that the different GoF tests, which ranked the probability distribution models differently, were normalized. Results show that, for each hydrometeorological data series, the best-fit probability distribution models were different for the different time scales (i.e., monthly, seasonal, and monthly). Our results corroborate those reported in the literature (see Li et al. 2013, and references therein). The evaporation data series was best fit by the Pearson system, the Lake Kariba water levels series was best fit by the Weibull family of probability distributions, and the rainfall series was best fit by the Weibull and the generalized Pareto probability distributions. To the best knowledge of the authors, this study is the first of its kind especially in southern Africa and therefore could contribute toward understanding the underlying processes driving changes in the hydroclimatic variables. Furthermore, the work presented in this paper has potential applications in such areas as simulation of precipitation concentration and distribution (as in weather generators) and water

Unauthenticated | Downloaded 08/05/21 09:27 PM UTC

resources management particularly in the Kariba catchment area and the larger Zambezi River basin as a result of (i) nonuniform distribution of a network of hydrometeorological stations; (ii) significant data gaps in the existing observations; and (iii) inherent impacts extreme events, climate change, and variability.

References

Chapman, T. G., 1997: Stochastic models for daily rainfall in the western Pacific. *Math. Comput. Simul.,* **43,** 351–358, doi:10.1016/S0378-4754(97)00019-0.

Chen, H., S. Guo, X. Ch-yu, and V. P. Singh, 2007: Historical temporal trends of hydro-climatic variables and runoff response to climate variability and their relevance in water resource management in the Hanjiang basin. *J. Hydrol.,* **344,** 171–184, doi:10.1016/j.jhydrol.2007.06.034.

De Luis, M., C. J. González-Hidalgo, M. Brunetti, and L. A. Longares, 2011: Precipitation concentration changes in Spain 1946–2005. *Nat. Hazards Earth Syst. Sci.,* **11,** 1259–1265, doi:10.5194/nhess-11-1259-2011.

Fathian, F., S. Morid, and E. Kahya, 2015: Identification of trends in hydrological and climatic variables in Urmia Lake basin, Iran. *Theor. Appl. Climatol.,* **119,** 443–464, doi:10.1007/s00704-014-1120-4.

Hosking, J. R. M., J. R. Wallis, and E. F. Wood, 1985: Estimation of the generalized extreme-value distribution by the method of probability weighted moments. *Technometrics,* **27,** 251–261, doi:10.1080/00401706.1985.10488049.

Huang, P., S. P. K. Hu, G. Huang, and R. Huang, 2013: Patterns of the seasonal response of tropical rainfall to global warming. *Nat. Geosci.,* **6,** 357–361, doi:10.1038/ngeo1792.

Jackson, I. J., 1977: *Climate, Water and Agriculture in the Tropics.* Longman, 248 pp.

Jöhnk, K. D., D. Straile, and W. Ostendorp, 2004: Water level variability and trends in Lake Constance in the light of the 1999 centennial flood. *Limnologica,* **34,** 15–21, doi:10.1016/S0075-9511(04)80017-3.

Kamruzzaman, M., S. Beecham, and A. V. Metcalfe, 2013: Climatic influences on rainfall and runoff variability in the southeast region of the Murray-Darling basin. *Int. J. Climatol.,* **33,** 291–311, doi:10.1002/joc.3422.

Lazaro, R., F. S. Rodrigo, L. Gutierrez, F. Domingo, and J. Puigdefafregas, 2001: Analysis of a 30-year rainfall record (1967-1997) in semi-arid SE Spain for implications on vegetation. *J. Arid Environ.,* **48,** 373–395, doi:10.1006/jare.2000.0755.

Levy, K. M., 1993: Intra-seasonal oscillations of convection over southern Africa. M.S. thesis, Oceanography Department, University of Cape Town, 228 pp.

Li, J., C. Sun, and F. F. Jin, 2013: NAO implicated as a predictor of Northern Hemisphere mean temperature multidecadal variability. *Geophys. Res. Lett.,* **40,** 5497–5502, doi:10.1002/2013GL057877.

Li, X.-Y., P.-J. Shi, Y.-L. Sun, J. Tang, and Z.-P. Yang, 2006: Influence of various in-situ rainwater harvesting methods on soil moisture and growth of *Tamarix ramosissima* in the semiarid loess region of China. *For. Ecol. Manage.,* **233,** 143–148, doi:10.1016/j.foreco.2006.06.013.

Li, Z., W. Z. Liu, X. C. Zhang, and F. L. Zheng, 2011: Assessing the site specific impacts of climate change on hydrology, soil erosion and crop yields in the Loess Plateau of China. *Climatic Change,* **105,** 223–242, doi:10.1007/s10584-010-9875-9.

Mannshardt-Shamseldin, E. C., R. L. Smith, S. R. Sain, L. O. Mearns, and D. Cooley, 2010: Downscaling extremes: A comparison of extreme value distributions in point-source and gridded precipitation data. *Ann. Appl. Stat.,* **4,** 484–502, doi:10.1214/09-AOAS287.

Matarira, C. H., and M. R. Jury, 1992: Contrasting meteorological structure of intra-seasonal wet and dry spells in Zimbabwe. *Int. J. Climatol.,* **12,** 165–176, doi:10.1002/joc.3370120205.

Unauthenticated | Downloaded 08/05/21 09:27 PM UTC

Mulenga, H. M., 1998: Southern African climate anomalies, summer rainfall and the Angola low. Ph.D. thesis, University of Cape Town, 232 pp.

Nicholson, S. E., 2000: The nature of rainfall variability over Africa on time scale of decades to millennia. *Global Planet. Change,* **26,** 137–158, doi:10.1016/S0921-8181(00)00040-0.

Ricci, V., 2005: Fitting distributions with R. Rep., 35 pp. [Available online at http://cran.r-project.org/doc/contrib/Ricci-distributions-en.pdf.]

Shang, H., J. Yan, M. Gebremichael, and S. M. Ayalew, 2011: Trend analysis of extreme precipitation in the northwestern highlands of Ethiopia with a case study of Debre Markos. *Hydrol. Earth Syst. Sci.,* **15,** 1937–1944, doi:10.5194/hess-15-1937-2011.

Tyson, P. D., 1984: The atmospheric modulation of extended wet and dry spells over South Africa, 1958-1978. *J. Climatol.,* **4,** 621–635, doi:10.1002/joc.3370040606.

——, 1986: *Climate Change and Variability in Southern Africa.* Oxford University Press, 220 pp.

Valli, M., S. S. Kotapati, and V. M. K. Iyyanki, 2013: Analysis of Precipitation Concentration Index and Rainfall Prediction in various Agro-Climatic Zones of Andhra Pradesh, India. *Int. Res. J. Environ. Sci.,* **2,** 53–61.

Wan, H., X. Zhang, and E. M. Barrow, 2005: Stochastic modelling of daily precipitation for Canada. *Atmos.–Ocean,* **43,** 23–32, doi:10.3137/ao.430102.

Wang, J., and X. Zhang, 2008: Downscaling and projection of winter extreme precipitation over North America. *J. Climate,* **21,** 923–937, doi:10.1175/2007JCLI1671.1.

Xu, C. C., Y. N. Chen, W. H. Li, and Y. P. Chen, 2006: Climate change and response of hydrology for recent several decades in the Tarim River Basin. *Chin. Sci. Bull.,* **51,** 21–30.

Xu, Z. X., Y. N. Chen, and J. Y. Li, 2004: Impact of climate change on water resources in the Tarim River Basin. *Water Resour. Manage.,* **18,** 439–458, doi:10.1023/B:WARM.0000049142.95583.98.

——, Z. Liu, G. Fu, and Y. Chen, 2010: Trends of major hydroclimatic variables in the Tarim River Basin during the past 50 years. *J. Arid Environ.,* **74,** 256–267, doi:10.1016/j.jaridenv.2009.08.014.

Zhao, G., G. Hormann, N. Fohrer, Z. Zhang, and J. Zhai, 2010: Streamflow trends and climate variability impacts in Poyang Lake basin, China. *Water Resour. Manage.,* **24,** 689–706, doi:10.1007/s11269-009-9465-7.

Earth Interactions is published jointly by the American Meteorological Society, the American Geophysical Union, and the Association of American Geographers. Permission to use figures, tables, and *brief* excerpts from this journal in scientific and educational works is hereby granted provided that the source is acknowledged. Any use of material in this journal that is determined to be ''fair use'' under Section 107 or that satisfies the conditions specified in Section 108 of the U.S. Copyright Law (17 USC, as revised by P.IL. 94-553) does not require the publishers' permission. For permission for any other from of copying, contact one of the copublishing societies.

Unauthenticated | Downloaded 08/05/21 09:27 PM UTC